Available online at www.sciencedirect.com
SCIENCE DIRECT
ELSEVIER
Journal of the European Ceramic Society 26 (2006) 1857–1860
ECERS
www.elsevier.com/locate/jeurceramsoc

Characterization of dielectric properties of oxide materials in frequency range from GHz to THz

Takashi Fujii *, Akira Ando, Yukio Sakabe

Murata Manufacturing Co., Ltd., Higashikoutari 1-10-1, Nagaokakyo, Kyoto 617-8555, Japan

Available online 28 November 2005

Abstract

We measured complex dielectric permittivity using THz time-domain spectroscopy (THz-TDS) to clarify the dielectric properties of oxide materials in a frequency range from GHz to THz. Piezoelectric and ferromagnetic oxide single crystals, such as quartz (SiO_2), zinc oxide (ZnO), Bi substituted rear-earth iron garnet (BiRIG), and $LiTaO_3$ (LT), were used. We obtained the complex dielectric permittivity of these materials in a frequency range from 100 GHz to 2 THz. The ε' and ε'' obtained for SiO_2 were in agreement with previous reports. We observed dielectric relaxation in ZnO crystal from 100 GHz to 1 THz, which originated from n-type conductivity. In the BiRIG, the values of the dielectric permittivity increased as the frequency increased, and the values of the dielectric permittivity with the magnetic field were smaller than those without the magnetic field throughout the measured frequency range. In a comparison between congruent $LiTaO_3$ (CLT) and stoichiometric $LiTaO_3$ (SLT), the ε_{33} of the CLT was very similar to that of the SLT, but a lot of difference was between the ε_{11} of evident CLT and SLT within the measured frequency region. We determined that the point defects had profound effect on the dielectric performance of the LT.

Keywords: THz-TDS; Dielectric properties; ZnO

1. Introduction

The frequency range from 800 MHz to 2 GHz has been used in developing wireless communication technology so far. New telecommunication systems in the planning stage, such as an intelligent traffic system (ITS), will use a higher range (from 30 to 300 GHz and over). Moreover, ubiquitous communication networks will be built in the near future using the frequency in a range from GHz to THz. However, the THz wave should be employed for medical and security technology. Therefore, clarifying the dielectric properties for electrical devices with regard to the frequency range from GHz to THz is important.

Coherent THz radiation has been obtained as a further development in the femtosecond pulse laser (fs laser), and thus, THz time-domain spectroscopy (THz-TDS) enables characterizing the dielectric properties ranging from GHz to THz. This method has the advantages of principle and convenience for measuring the complex dielectric permittivity in this frequency range in comparison with other methods, such as far-infrared Fourier transform spectroscopy and the Hacky–Coleman method.[1–3]

In this paper, we report THz-TDS measurements of piezoelectric and ferromagnetic oxide single crystals to clarify material performance and the complex dielectric permittivity within the range of the GHz and THz wave (from 100 GHz to 2 THz).

2. Experimental

We prepared Z-plate quartz (Z-SiO_2), Z-plate zinc oxide (Z-ZnO), (1 1 1) Bi substituted rear-earth iron garnet (BiRIG), Y-plate congruent $LiTaO_3$ (Y-CLT), and Y-plate stoichiometric $LiTaO_3$ (Y-SLT) for measurement samples. The Z-SiO_2 and Z-ZnO were grown by the hydrothermal growth method.[4] The BiRIG (the material for an optical isolator made by the Mitsubishi Gas Chemical Company Inc. in Japan) was grown by the liquid phase epitaxy method. The Y-CLT was grown by the conventional Czochralski method, and the Y-SLT was grown by double-crucible Czochralski method.[5]

We used a THz-TDS apparatus (Jspec-2001 made by the Mutsumi Corporation in Japan) with a femtosecond Ti-sapphire plus laser (MaiTai made by the Spectra Physics Corporation in the USA).[3] Fig. 1 shows a schematic illustration of the optical configuration in the apparatus. After the light of the fs laser is divided into two optical paths by a beam splitter, one is guided to an emitter, and the other is guided to a detector, respectively. Both

* Corresponding author.

0955-2219/$ – see front matter © 2005 Elsevier Ltd. All rights reserved.
doi:10.1016/j.jeurceramsoc.2005.09.094

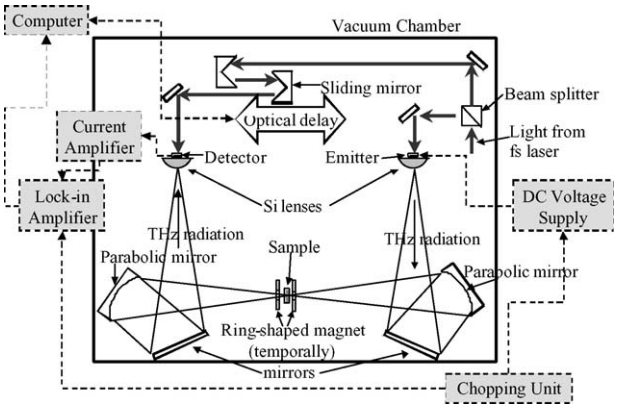

Fig. 1. Schematic illustration of optical configuration in THz-TDS apparatus. The bold arrows indicate the fs laser light, and the broken lines show the electrical flow. The ring-shaped permanent magnets were attached when BiRIG was measured.

Table 1
Experimental conditions

Sample	Thickness (mm)	Aperture (mm in diameter)
Z-SiO_2	0.407	8
Z-ZnO	0.516	8
(1 1 1) BiRIG	0.236	8
Y-CLT	0.264	5
Y-SLT	0.732	5

the emitter and detector consisted of a photoconductive antenna made of low-temperature grown GaAs. The THz electromagnetic waves radiate from the emitter antenna. The measuring frequency ranges from 60 GHz to 2.8 THz, and the frequency resolution is 2 GHz. This apparatus was configured to transmit THz radiation through the samples.

The experimental conditions are listed in Table 1. The optical aperture was 5 mm or 8 mm in diameter, and we measured the materials at room temperature. We measured ε_{11} in Z-SiO_2 and Z-ZnO and ε_{11} and ε_{33} in Y-CLT and Y-SLT. In the BiRIG, we measured the dielectric permittivity with and without an applied external magnetic field. A pair of ring-shaped permanent magnets was temporally arranged along the THz radiative direction, as shown in Fig. 1. The direction of the magnetic field was parallel to the ⟨1 1 1⟩ direction in the BiRIG, and the magnitude of the field was 190 mT.

3. Results and discussions

Fig. 2 shows the results of the complex dielectric permittivity (ε'_{11} and ε''_{11}) of the Z-SiO_2 in the range from 80 GHz to 1.8 THz. The ε'_{11} was 4.45 for the measuring frequency, and the ε''_{11} was about 0.03. The ε'^{T}_{11} at 1 KHz was 4.52, so the dielectric permittivity of quartz was uniform in the range from KHz to THz. These results were consistent with a previous report.[6]

The results of the dielectric permittivity for Z-ZnO crystal are shown in Fig. 3. The ε'_{11} was 7.9 and was constantly within the measuring frequency range. The ε'^{T}_{11} at 1 KHz was 8.4 and this value was slightly bigger than the measuring values. However,

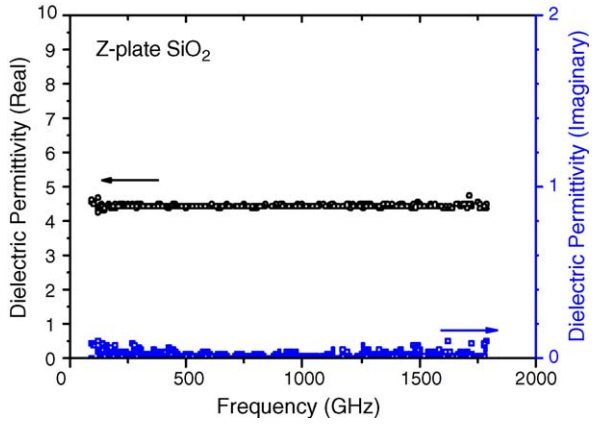

Fig. 2. Real (ε'_{11}) and imaginary (ε''_{11}) parts of complex dielectric permittivity of Z-SiO_2. The open circles indicate ε'_{11} and the open squares indicate ε''_{11}.

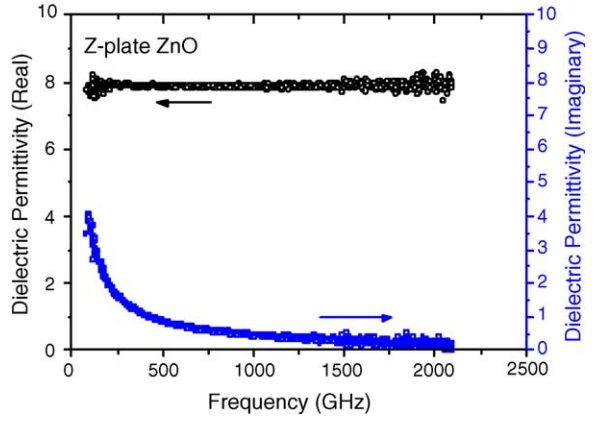

Fig. 3. Real (ε'_{11}) and imaginary (ε''_{11}) parts of complex dielectric permittivity of Z-ZnO. The open circles indicate ε'_{11} and the open squares indicate ε''_{11}.

the ε''_{11} decreased as the frequency increased. Also, the dielectric relaxation from 100 GHz to 1 THz was observed. This shows Drude effect, which is in ZnO crystal of n-type conductivity.

The results of the (1 1 1) BiRIG with and without the external magnetic field are shown in Figs. 4 and 5, respectively. The BiRIG is ferromagnetic crystal, and the magnetism axis is along

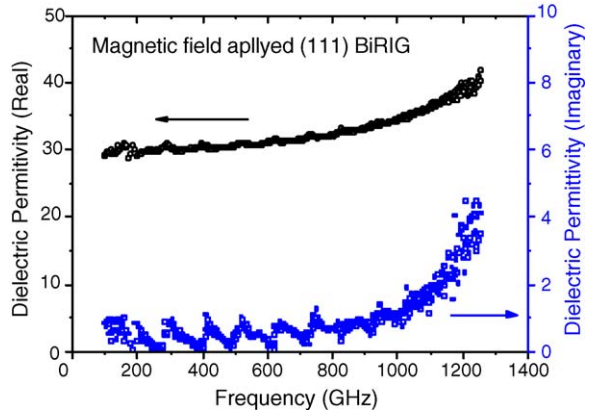

Fig. 4. Real and imaginary parts of complex dielectric permittivity of (1 1 1) BiRIG with external magnetic field. The open circles indicate the real part, and the open squares indicate the imaginary part.

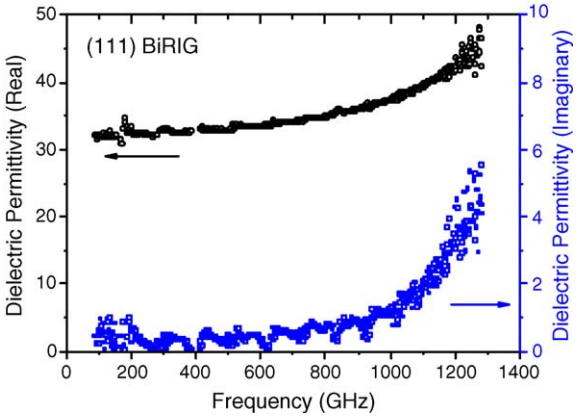

Fig. 5. Real and imaginary parts of complex dielectric permittivity of (1 1 1) BiRIG without external magnetic field. The open circles indicate the real part and the open squares indicate the imaginary part.

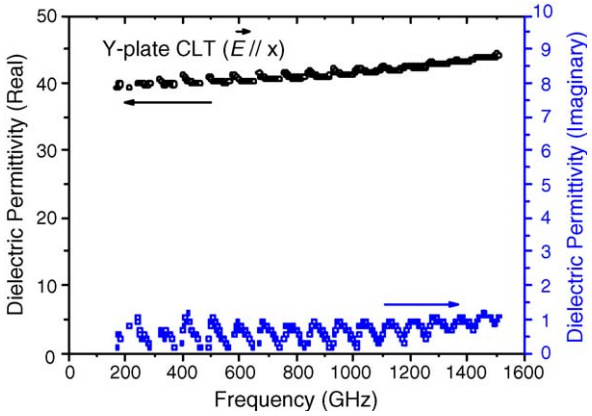

Fig. 7. Real (ε'_{11}) and imaginary (ε''_{11}) parts of complex dielectric permittivity of Y-CLT. The open circles indicate ε'_{11} and the open squares indicate ε''_{11}.

the ⟨1 1 1⟩ direction. The sample is in multi-domain state without a magnetic field, while single domain state appears in 190 mT of the magnetic field. The crystal structure of the BiRIG is cubic system and then, the values of the dielectric permittivity in this measurement could be estimated to ε_{11} in Fig. 3. No difference could be found between with and without the magnetic field for an upward tendency of the dielectric permittivity. But the values of the dielectric permittivity with the magnetic field were smaller than those without the magnetic field within the measured frequency range. In regard to these results, we assume the following:

1. The symmetrical change due to applying the magnetic field caused the difference in the dielectric permittivity.
2. The existence of the magnetic domain affected the dielectric permittivity.
3. The transmittance of the electromagnetic waves varied owing to the Faraday effect.

Confirmation of one from this possibility needs further studies.

As is shown in Figs. 6 and 7, which correspond to ε_{33} and ε_{11}, respectively, the ε'_{33} and ε'_{11} were about 42 and 40 at 400 GHz. $LiTaO_3$ (LT) is the ferroelectric material. The ε'^{S}_{33} and ε'^{S}_{11} at 100 KHz are 42.8 and 38.1, respectively, and both values gradually increased as the frequency increased. Our obtained data was almost the same as in a previous report.[7]

In Figs. 4–7, periodic spectra along the horizontal axis are observed. This phenomenon was due to the mismatch of sample thickness and never corresponded to the variations of the dielectric permittivity. Accordingly, this periodic profile can be avoided by adjusting the sample thickness.

In Y-SLT, the values of ε'_{33} and ε'_{11} were about 42 and 38 at 400 GHz, respectively, as is shown in Figs. 8 and 9. Moreover, the ε'_{11} in Fig. 9 was permittivity in the measured frequency range. In a comparison between the CLT and SLT, the ε_{33} of the CLT was very similar to that of SLT, but there was a lot of difference between the ε_{11} of the CLT and SLT. As is well-known, the CLT has a lot of point defects in the crystal, as compared with the SLT. Although the dielectric permittivity of the CLT was little different from those of the SLT at 100 KHz, much distinction existed in our obtained results. Furthermore, the performance of the SLT was reported to exceed that of the CLT in the optical region.[8] We determined that the point defects in the crystal had a profound effect on the dielectric performance of the crystal at this frequency range.

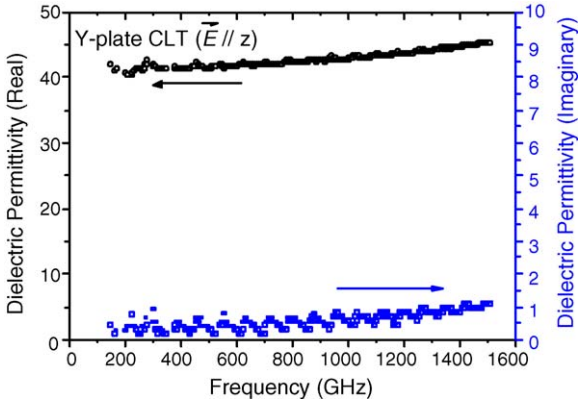

Fig. 6. Real (ε'_{33}) and imaginary (ε''_{33}) parts of complex dielectric permittivity of Y-CLT. The open circles indicate ε'_{33} and the open squares indicate ε''_{33}.

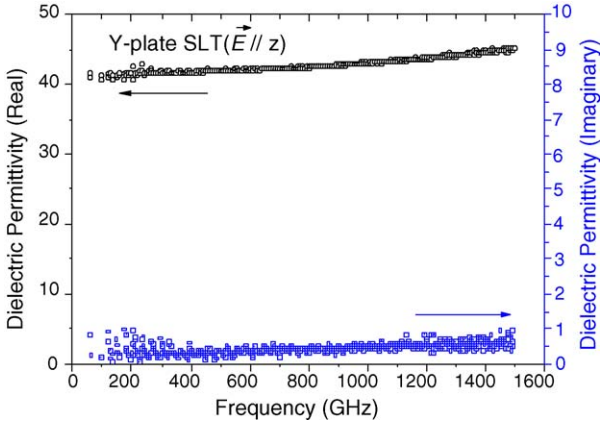

Fig. 8. Real (ε'_{33}) and imaginary (ε''_{33}) parts of complex dielectric permittivity of Y-SLT. The open circles indicate ε'_{33} and the open squares indicate ε''_{33}.

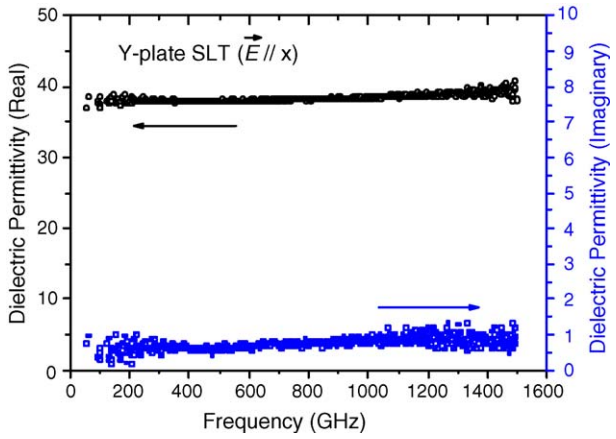

Fig. 9. Real (ε'_{11}) and imaginary (ε''_{11}) parts of complex dielectric permittivity of Y-SLT. The open circles indicate ε'_{11} and the open squares indicate ε''_{11}.

4. Conclusion

We measured piezoelectric and ferromagnetic oxide single crystals, such as Z-SiO_2, Z-ZnO, (1 1 1) BiRIG, Y-CLT, and Y-SLT to clarify the dielectric properties of oxide materials in a frequency range from GHz to THz. We used THz-TDS, and we obtained the complex dielectric permittivity of these materials in a frequency range from 100 GHz to 2 THz. The ε' and ε'' obtained for Z-SiO_2 were in agreement with previous reports. We observed dielectric relaxation in ZnO from 100 GHz to 1 THz, which originated from n-type conductivity. In the BiRIG, though there was no difference from an upward tendency of the dielectric permittivity with and without a magnetic field, the values of the dielectric permittivity with the magnetic field were smaller than those without it throughout the measured frequency range. In a comparison between CLT and SLT, the ε_{33} of the CLT was very similar to that of the SLT, but a lot of difference was evident between the ε_{11} of the CLT and SLT within the measured frequency region. We determined that the point defects in the crystal had profound effect on the dielectric performance of the crystal. Analyzing the dielectric properties in the frequency range from GHz to THz is more important development in a high frequency application because THz-TDS is useful for measuring in this frequency range.

Acknowledgment

We owe a great deal of gratitude to Prof. Mitsuo Wada Takeda of Shinshu University for his useful suggestions and advice regarding the THz-TDS measurement.

References

1. Exter, M. and Grischkowsky, D., Optical and electronic properties of doped silicon from 0.1 to 2 THz. *Appl. Phys. Lett.*, 1990, **56**, 1694–1696.
2. Kojima, S., Tsunura, N., Takeda, M. W. and Nishizawa, S., Far-infrared phonon-polariton dispersion probed by terahertz time-domain spectroscopy. *Phys. Rev. B*, 2003, **67**, 035102–035107.
3. Fujii, T., Ando, A. and Sakabe, Y., Dielectric characteristics of ferroelectric materials in submillimeter-wave regions. *Jpn. J. Appl. Phys.*, 2004, **43**, 6765–6768.
4. Ohshima, E., Ogino, H., Niikura, I., Maeda, K., Sato, M., Ito, M. *et al.*, Growth of 2-in-size bulk ZnO single crystals by the hydrothermal method. *J. Cryst. Growth*, 2004, **260**, 166–170.
5. Furukawa, Y., Kitamura, K., Suzuki, E. and Niwa, K., Stoichiometric $LiTaO_3$ single crystal growth by double-crucible Czochralski method using automatic power. *J. Cryst. Growth*, 1999, **197**, 889–895.
6. Grischkoswsky, D., Keiding, S., Exter, M. and Fattinger, C., Far-infrared time-domain spectroscopy with terahertz beams of dielectrics and semiconductors. *J. Opt. Soc. Am. B*, 1990, **7**, 2006–2015.
7. Kojima, S., Kitahara, H., Nishizawa, S. and Takeda, M. W., Dielectric properties of ferroelectric lithium tantalate crystal studied by terahertz time-domain spectroscopy. *Jpn. J. Appl. Phys.*, 2003, **42**, 6238–6241.
8. Hatanaka, T., Nakamura, K., Taniuchi, T., Ito, H., Furukawa, Y. and Kitamura, K., Quasi-phase matched optical parametric oscillation with periodically poles stoichiometric $LiTaO_3$. *Opt. Lett.*, 2000, **25**, 651–653.